Immunity

Article

Retinoic-Acid-Receptor-Related Orphan Nuclear Receptor Alpha Is Required for Natural Helper Cell Development and Allergic Inflammation

Timotheus Y.F. Halim,[1,2] Aric MacLaren,[1] Mark T. Romanish,[1] Matthew J. Gold,[3] Kelly M. McNagny,[3] and Fumio Takei[1,2,4,*]

[1]Terry Fox Laboratory, British Columbia Cancer Agency, Vancouver, BC V5Z 1L3, Canada
[2]Genetics Graduate Program, College for Interdisciplinary Studies, University of British Columbia, Vancouver, BC V6T 1Z2, Canada
[3]Biomedical Research Centre, University of British Columbia, Vancouver, BC V6T 1Z3, Canada
[4]Department of Pathology and Laboratory Medicine, University of British Columbia, Vancouver, BC V6T 2B5, Canada
*Correspondence: ftakei@bccrc.ca
http://dx.doi.org/10.1016/j.immuni.2012.06.012

SUMMARY

Natural helper (NH) cells are innate lymphoid cells (ILCs) that produce T helper-2 (Th2)-cell-type cytokines in the lung- and gut-associated lymphoid tissues. Currently, the lineage relationship between NH cells in different tissues and between NH cells and interleukin-22 (IL-22)-producing retinoic-acid-receptor-related orphan receptor (ROR)γt-positive ILCs is unclear. Here, we report that NH cells express RORα, but not RORγt. RORα-deficient, but not RORγt-deficient, mice lacked NH cells in all tissues, whereas all other lymphocytes, including RORγt[+] ILCs, were unaffected. NH-cell-deficient mice generated by RORα-deficient bone-marrow transplantation had normal Th2 cell responses but failed to develop acute lung inflammation in response to protease allergen, thus confirming the essential role of NH cells in allergic lung inflammation. We have also identified RORα-dependent NH cell progenitors in the bone marrow. Thus, all NH cells belong to a unique RORα-dependent cell lineage separate from other lymphoid cell lineages.

INTRODUCTION

Natural helper (NH) cells, also termed nuocytes (Neill et al., 2010), multipotent progenitor type 2 (MPP[type2]) cells (Saenz et al., 2010), type 2 innate lymphoid (ILC2) cells (Mjösberg et al., 2011), and innate helper type 2 (Ih2) cells (Price et al., 2010), are a recently identified type of innate lymphocyte in mucosal tissues and are capable of producing large amounts of T helper-2 (Th2)-cell-type cytokines. NH cells are activated by stroma-derived IL-33, IL-25, or thymic stromal lymphopoietin (TSLP) and rapidly produce IL-5 and IL-13 (Halim et al., 2012); they have been implicated in the expulsion of helminths from the gut (Neill et al., 2010; Price et al., 2010; Saenz et al., 2010), activation of B1 B cells in the peritoneum (Moro et al., 2010), airway hyperreactivity and tissue repair in the lungs after influenza infection (Chang et al., 2011; Monticelli et al., 2011), and

protease-allergen-induced lung inflammation (Halim et al., 2012). Although the precise relationship between NH cells in the lung- and gut-associated lymphoid tissues is still unclear, all NH cells are thought to belong to a larger family of innate lymphocytes (ILCs), which include natural killer (NK) cells and ILCs expressing retinoic-acid-receptor-related orphan nuclear receptor (ROR)γt (Spits and Cupedo, 2012). Although NH cells and RORγt[+] ILCs are similar in cell-surface-marker expression, they markedly differ in their functions. The former produce Th2-cell-type-derived cytokines, whereas the latter produce IL-22 and IL-17. The development of NH cells, RORγt[+] ILCs, and NK cells is dependent on the transcription factor Id2 (Monticelli et al., 2011; Moro et al., 2010); RORγt[+] ILC development is also dependent on RORγt encoded by *Rorct* (Eberl et al., 2004; Sanos et al., 2009; Sawa et al., 2010). Given that we previously found that lung NH cells from naive C57BL/6 mice exhibit a high expression of *Rora,* which encodes another member of the ROR family of transcription factors, namely RORα, but not *Rorc* (Halim et al., 2012), we now have examined NH cells and RORγt[+] ILCs in various tissues of RORα-deficient and RORγt-deficient mice. We report here that RORα-deficient mice have almost no NH cells in the lungs or small and large intestines, but they have normal numbers of RORγt[+] ILCs in these tissues. Conversely, RORγt-deficient mice lack RORγt[+] ILCs but have normal NH cells. We have also identified in the bone marrow (BM) immature NH (iNH) cells that develop into mature NH cells in the lungs and gut. NH-cell-deficient mice have Th2 cells but do not get allergic lung inflammation in response to protease-allergen stimulation.

RESULTS

NH Cells Express *Rora* and Can Be Distinguished from RORγt[+] ILCs by Sca-1 and c-Kit Expression

As we previously reported (Halim et al., 2012), NH cells in naive C57BL/6 (B6) mouse lungs were readily identified by their distinct pattern of cell-surface-marker expression: lineage-marker-negative (Lin^{−}) CD127^{+}CD25^{+}Sca-1^{hi}c-Kit^{lo} (Figure 1A, top). They expressed the IL-33 receptor T1/ST2 (ST2) chain, but not the chemokine receptor CCR6, which is known to be expressed on RORγt^{+} ILCs. In the small intestine, large intestine, and mesenteric lymph nodes (MLNs), Lin^{−}CD127^{+}CD25^{+} cells
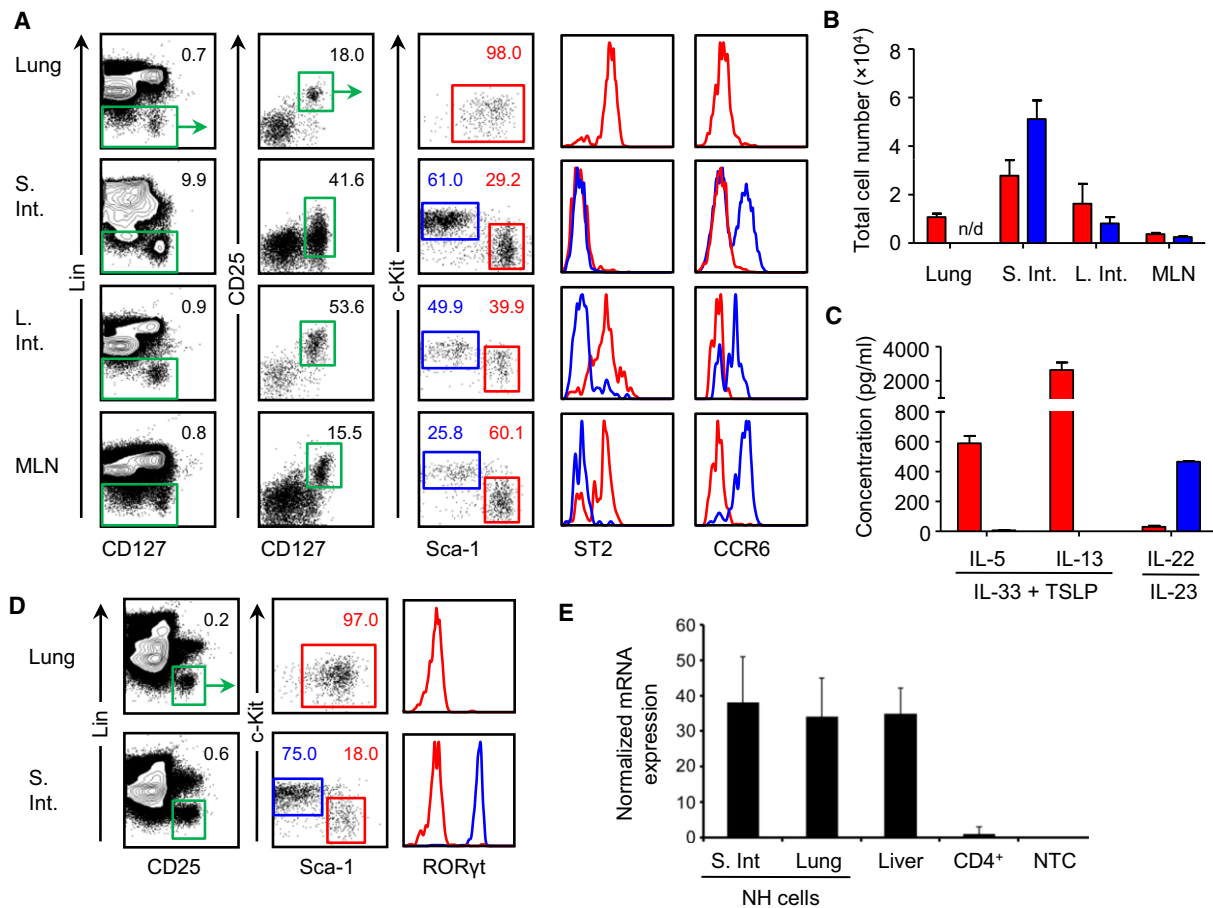
Figure 1. *Rora*- and *Rorct*-Expressing Innate Lymphocyte Subsets in Naive WT Mice

(A) Cells from the lungs, small intestine (S. Int.), large intestine (L. Int.), and mesenteric lymph nodes (MLNs) were analyzed by flow cytometry. Live (PI$^-$) leukocytes (CD45$^+$) were gated first, and lineage (Lin)-negative cells were gated (green box) and analyzed for CD127 and CD25 expression. CD25$^+$CD127$^+$ cells were then gated (green box) and analyzed for Sca-1 and c-Kit expression. Sca-1$^+$c-Kit^{lo} cells (red) and Sca-1$^-$c-Kit$^+$ cells (blue) were gated and analyzed for CCR6 and ST2 expression. Red and blue histograms correspond to the cells gated by the boxes in the same colors in the plots.

(B) Absolute numbers (per mouse) of Lin$^-$CD127$^+$CD25$^+$Sca-1$^+$c-Kit^{lo} cells (red) and Lin$^-$CD127$^+$CD25$^+$Sca-1$^-$c-Kit$^+$ cells (blue) in indicated tissues were calculated from the total number of CD45$^+$ live cells and the frequencies of individual cell populations determined in (A).

(C) Lin$^-$CD127$^+$CD25$^+$Sca-1$^+$c-Kit^{lo} cells (red) and Lin$^-$CD127$^+$CD25$^+$Sca-1$^-$c-Kit$^+$ cells (blue) were FACS purified from the small intestine and stimulated in vitro with IL-33 plus TSLP or IL-23 plus IL-7 for 3 days, and the indicated cytokines in culture supernatant were analyzed by ELISA.

(D) Lin$^-$CD25$^+$Sca-1$^+$c-Kit^{lo} NH cells (red) and/or Lin$^-$CD25$^+$Sca-1$^-$c-Kit$^+$ ILCs (blue) in the indicated tissues were stained for intracellular RORγt. All cells were first gated for live (eFluor780$^-$) leukocytes (CD45$^+$).

(E) NH cells (Lin$^-$CD127$^+$CD25$^+$Sca-1$^+$c-Kit^{lo} cells) were purified from the small intestine (gut) and lungs; RNA was extracted, converted to cDNA, and subjected to qPCR analysis for *Rora* mRNA expression. Relative expression values are normalized to endogenous β-actin and are shown relative to *Rora* expression in CD4$^+$ T cells. No template control (NTC) was used. Error bars represent the mean of three independent experiments ± standard deviation (SD).

Data are representative of at least three independent experiments (mean and standard error of the mean [SEM] in B and C) (see also Figure S1).

could be divided into two clearly distinguishable populations, Sca-1$^-$c-Kit$^+$ and Sca-1^{hi}c-Kit^{lo}. The former expressed CCR6, but not ST2, whereas the latter was CCR6$^-$ST2$^+$; the only exception was those in the small intestine, which did not express ST2 (Figure 1A, second row). Although both Lin$^-$CD127$^+$CD25$^+$ Sca-1$^-$c-Kit$^+$ and CD127$^+$CD25$^+$Sca-1^{hi}c-Kit^{lo} cells (gated by blue and red boxes, respectively, in Figure 1A) were found in the intestines and MLNs in comparable numbers, the former population was not detected in the lungs (Figures 1A and 1B). We purified the two cell populations from the small intestine and stimulated them with either IL-33 plus TSLP or IL-23. The Sca-1^{hi}c-Kit^{lo} subset was very similar to lung NH cells in our pre-

vious study (Halim et al., 2012) and produced IL-5 and IL-13 in response to IL-33 plus TSLP but did not produce a substantial amount of IL-22 in response to IL-23 (Figure 1C, red bars). Therefore, this population most likely consisted of NH cells. In contrast, the Sca-1$^-$c-Kit$^+$ subset produced IL-22 in response to IL-23 but did not produce IL-5 or IL-13 upon stimulation with IL-33 plus TSLP (Figure 1C, blue bars), indicating that this population most likely contained RORγt$^+$ ILCs, but not NH cells. Lung NH cells did not produce IL-22 (Figure S1A, available online). Intracellular staining confirmed that all Lin$^-$CD127$^+$CD25$^+$ Sca-1$^-$c-Kit$^+$ cells in the small intestine were RORγt$^+$ and that CD127$^+$CD25$^+$Sca-1^{hi}c-Kit^{lo} cells were RORγt$^-$ (Figure 1D). No
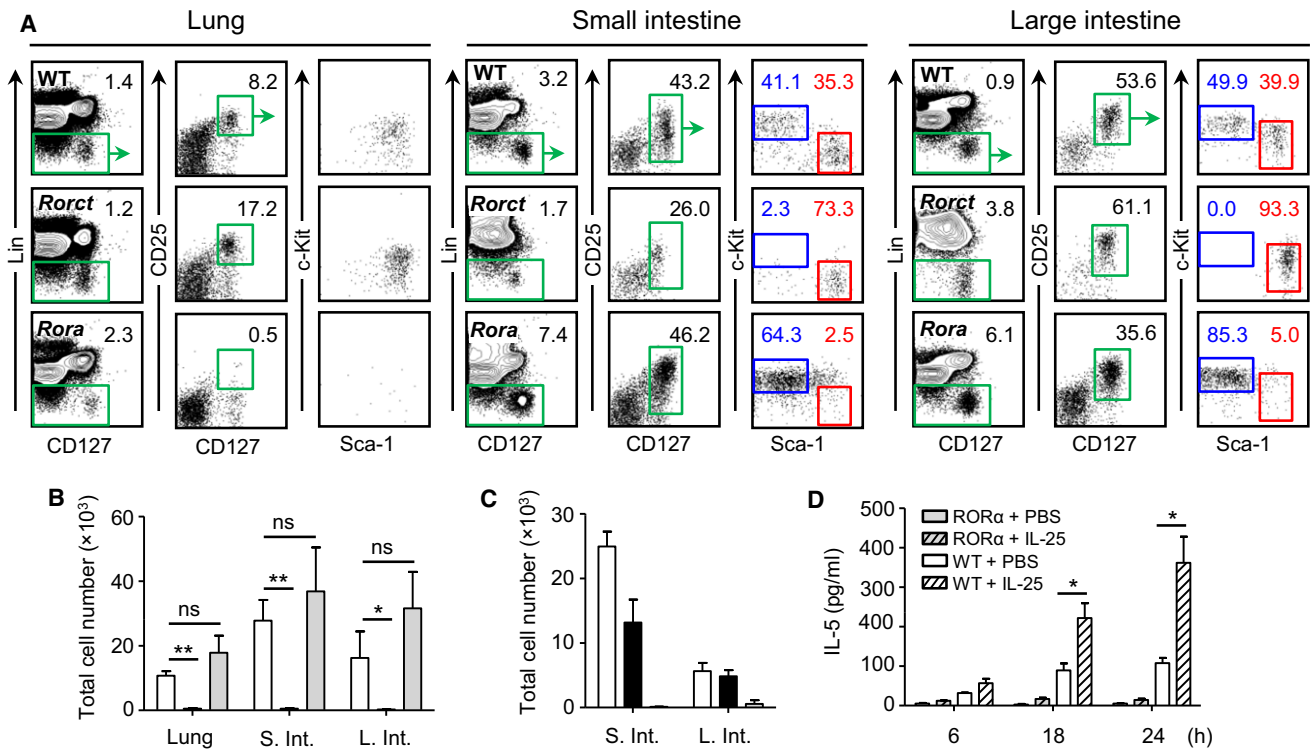
Figure 2. *Rora^{sg/sg}* Mice Are Deficient in NH Cells, but Not ILCs

(A) Cells were isolated from the lungs, small intestine, and large intestine of WT, *Rora^{sg/sg}*, *Rorct^{−/−}* mice and analyzed by flow cytometry as in Figure 1. Lin⁻CD127⁺CD25⁺ cells in the indicated tissues were gated (green boxes), and NH cells (red) and RORγt⁺ ILCs (blue) were identified by Sca-1⁺c-Kit^{lo} and Sca-1⁻c-Kit⁺, respectively. Numbers show the percentages of cells in the gates. Live (PI⁻) CD45⁺ leukocytes were analyzed.

(B) Total numbers (per mouse) of NH cells in the indicated tissues of WT (white), *Rora^{sg/sg}* (black), and *Rorct^{−/−}* (gray) mice were calculated from their percentages among CD45⁺ cells and the total numbers of CD45⁺ cells in each tissue.

(C) Total numbers of RORγt⁺ ILCs per mouse in indicated tissues were calculated as in (B).

(D) Small-intestine explant cultures from indicated mouse strains were stimulated with PBS (ctrl) or IL-25 and analyzed for cytokine production at the indicated time points.

*p < 0.05, **p < 0.001 (two-tailed Student's t test). Data are representative of at least three independent experiments (mean and SEM in B–D) (see also Figure S2).

RORγt⁺ Lin⁻CD25⁺ cells were found in naive mouse lungs. Thus, normal mouse lungs seemed to have no detectable RORγt⁺ ILCs. This is consistent with our previous microarray analysis of global gene expression in lung NH cells, which showed no detectable *Rorc* expression (Halim et al., 2012) (Figure S1B). Instead, they expressed increased transcript of *Rora*, which encodes RORα, another member of the ROR family of nuclear receptors. The expression of *Rora* in both lung and gut NH cells was confirmed by quantitative PCR (qPCR) (Figure 1E).

RORα-Deficient Mice Do Not Have Functional NH Cells

The *staggerer* mutation (*Rora^{sg/sg}*) deletes *Rora*. To test the effects of RORα deficiency, we compared NH cells, RORγt⁺ ILCs, and other lymphocytes in *Rora^{sg/sg}*, *Rorct^{−/−}*, and wild-type (WT) B6 mice. The amount of Lin⁻CD127⁺CD25⁺Sca-1^{hi}c-Kit^{lo} NH cells was much lower in the lungs and small and large intestines of *Rora^{sg/sg}* mice than in those of WT or *Rorct^{−/−}* mice (Figure 2A). Conversely, RORγt⁺ ILCs (Lin⁻CD127⁺CD25⁺ Sca-1⁻c-Kit⁺) were undetectable in *Rorct^{−/−}* mice, as expected (Spits and Di Santo, 2011), but these mice did have normal NH cells. The absolute number of NH cells in *Rora^{sg/sg}* mice was severely reduced to almost undetectable numbers in all tissues

examined (Figure 2B). Heterozygous *Rora^{sg/+}* mice had normal NH cell numbers (Figures S2A and S2B). The number of RORγt⁺ ILCs was also moderately lower in the small intestine, but not in the large intestine, of *Rora^{sg/sg}* mice than in that of WT mice, whereas they were almost undetectable in the small and large intestines of *Rorct^{−/−}* mice (Figure 2C). It should be noted that *Rora^{sg/sg}* mice in this analysis were only 3 weeks old and notably smaller than WT and *Rorct^{−/−}* mice. These data further confirm the gating strategy for identifying NH cells and RORγt⁺ ILCs in Figure 1, and they highlight the importance of using Sca-1 and c-Kit for differentiating between the two innate lymphocyte populations in the gut.

The lungs of *Rora^{sg/sg}* mice had a distinct Lin⁻CD127⁺CD25⁻ population, possibly representing NH cells with a slightly changed phenotype. However, these cells did not produce Th2-cell-type cytokines when purified by flow cytometry and stimulated in vitro (data not shown). To further exclude the possibility of functional but phenotypically different NH cells being present in *Rora^{sg/sg}* mice, we stimulated organ explants from WT and *Rora^{sg/sg}* mouse small intestines with IL-25 (Figure 2D). Explant cultures prepared from WT mice produced significantly more IL-5 in response to IL-25 than did those from *Rora^{sg/sg}*
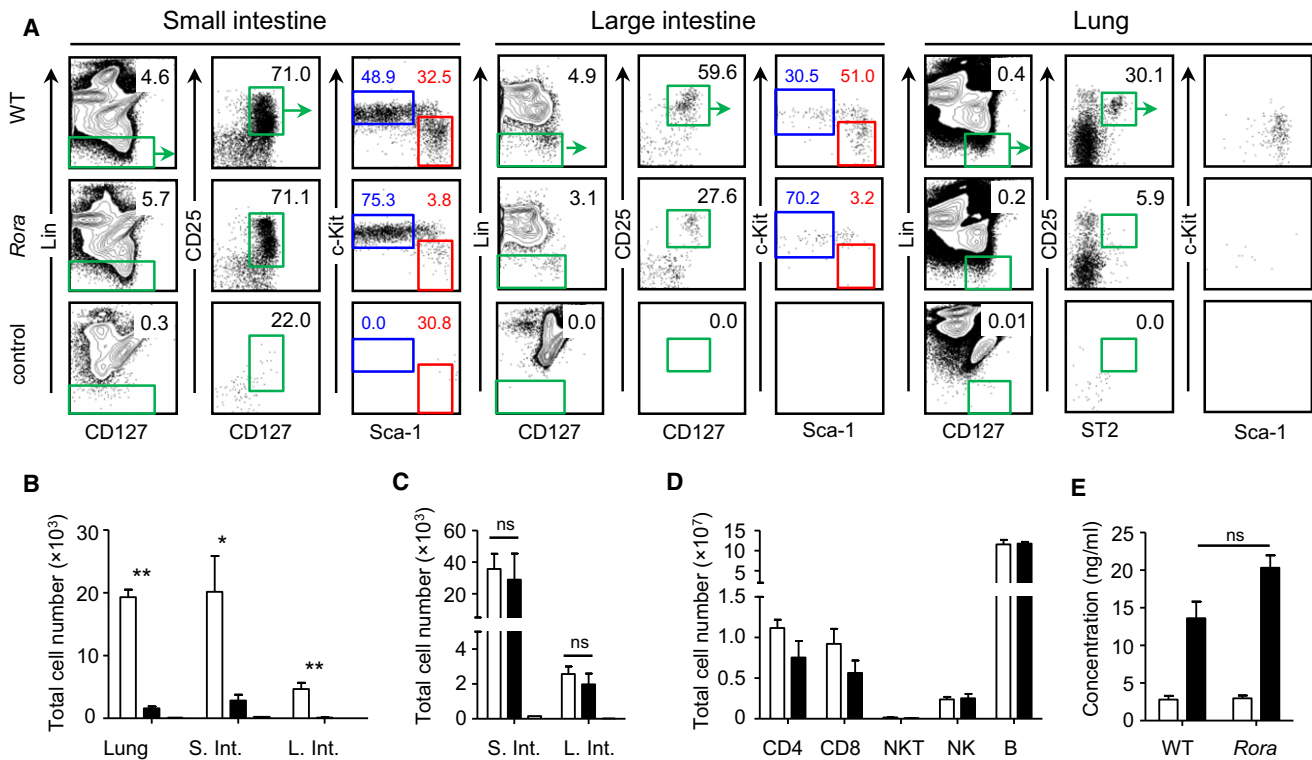
Figure 3. *Rora* Deficiency Affects NH Cell Development

(A) $Rag2^{-/-}Il2rg^{-/-}$ (RGC) mice (control) were reconstituted with $Rora^{sg/sg}$ or WT BM and were subjected to FACS analysis for Lin⁻CD127⁺CD25⁺Sca-1⁺c-Kit^lo NH cells (red) and Lin⁻CD127⁺CD25⁺Sca-1⁻c-Kit⁺ ILCs (blue) in the indicated tissues. Numbers show the percentages of cells in the gates. Live (PI⁻) CD45⁺ leukocytes were analyzed.

(B and C) Absolute numbers (per mouse) of NH cells (B) and RORγt⁺ ILCs (C) in WT mice (white), $Rora^{sg/sg}$ BMT mice (black), or RGC control mice (gray) were calculated in the indicated tissues.

(D) Other leukocyte subsets in WT (white) or $Rora^{sg/sg}$ BMT (black) mice were identified by flow cytometry, and absolute numbers in the spleen were calculated.

(E) CD4⁺ T cells were purified from the spleens of RGC mice reconstituted with WT or $Rora^{sg/sg}$ BM and stimulated under Th2-inducing conditions for 5 days. On day 5, one million cells were stimulated for 24 hr, and supernatant was analyzed for IL-5 (white bars) or IL-13 (black bars) production.

*p < 0.05, **p < 0.001 (two-tailed Student's t test). Data are representative of at least three independent experiments (mean and SEM in B–E) (see also Figure S3).

mice, which produced almost none. When stimulated with IL-23, WT and $Rora^{sg/sg}$ explants produced comparable amounts of IL-22 (Figure S2C). We conclude that $Rora^{sg/sg}$ mice do not have functional NH cells but do have normal RORγt⁺ ILCs.

### *Rora^{sg/sg}* BM-Transplanted Mice Are NH Cell Deficient but Have Functional Th2 Cells and RORγt⁺ ILCs

RORα plays a critical role in the development of Purkinje cells in the mouse cerebellum (Gold et al., 2003) and cones in the retina (Fujieda et al., 2009). RORα-deficient homozygous *staggerer* ($Rora^{sg/sg}$) mice have severe neurological defects and do not survive long past weaning. $Rora^{sg/sg}$ mice also have a runty phenotype, exhibit significantly smaller spleens and thymi, and have reduced numbers of lymphocytes (Bakalian et al., 1992). To determine whether the NH cell deficiency in $Rora^{sg/sg}$ mice is due to the runty phenotype of the mice or to intrinsic effects of RORα on NH cell development, we transplanted $Rora^{sg/sg}$ or WT whole BM into sublethally irradiated lymphocyte-deficient $Rag2^{-/-}Il2rg^{-/-}$ (RGC) mice and analyzed lymphocytes in the mice after 8–16 weeks. NH (Lin⁻CD127⁺CD25⁺Sca-1^hic-Kit^lo) cells were readily detected in the lungs, small intestine, and large intestine of RGC mice receiving WT

BM transplantation (WT BMT mice) (Figure 3A, top row). RORγt⁺ ILCs (CD127⁺CD25⁺Sca-1⁻c-Kit⁺) were also detected in the small and large intestines, but not in the lungs, of those mice. On the other hand, very few, if any, NH cells were found in the intestines and lungs of RGC mice injected with $Rora^{sg/sg}$ BM ($Rora^{sg/sg}$ BMT mice) (Figure 3A, middle row). RGC mice without BMT (Figure 3A, bottom row) did not have NH cells or other lymphocytes. The absolute numbers of NH cells in all tissues examined were significantly lower in $Rora^{sg/sg}$ BMT mice than in WT BMT mice (Figure 3B), whereas the absolute numbers of RORγt⁺ ILCs were not significantly different between those mice (Figure 3C). The two groups of mice also had comparable numbers of CD4⁺ T, CD8⁺ T, NK T (NKT), NK, and B cells in the spleen, indicating that RORα deficiency had no effect on the development of other lymphocytes (Figure 3D). We also isolated spleen CD4⁺ T cells from these mice and stimulated them to induce Th2 cell differentiation. $Rora^{sg/sg}$ BM-derived CD4⁺ T cells produced the same amounts of IL-5 and IL-13 as did WT BM-derived CD4⁺ T cells (Figure 3E), indicating that RORα deficiency had no significant effects on Th2 cell differentiation.

We also transplanted RORα-deficient BM into lethally irradiated C57BL/6-Pep3b mice and analyzed the development of
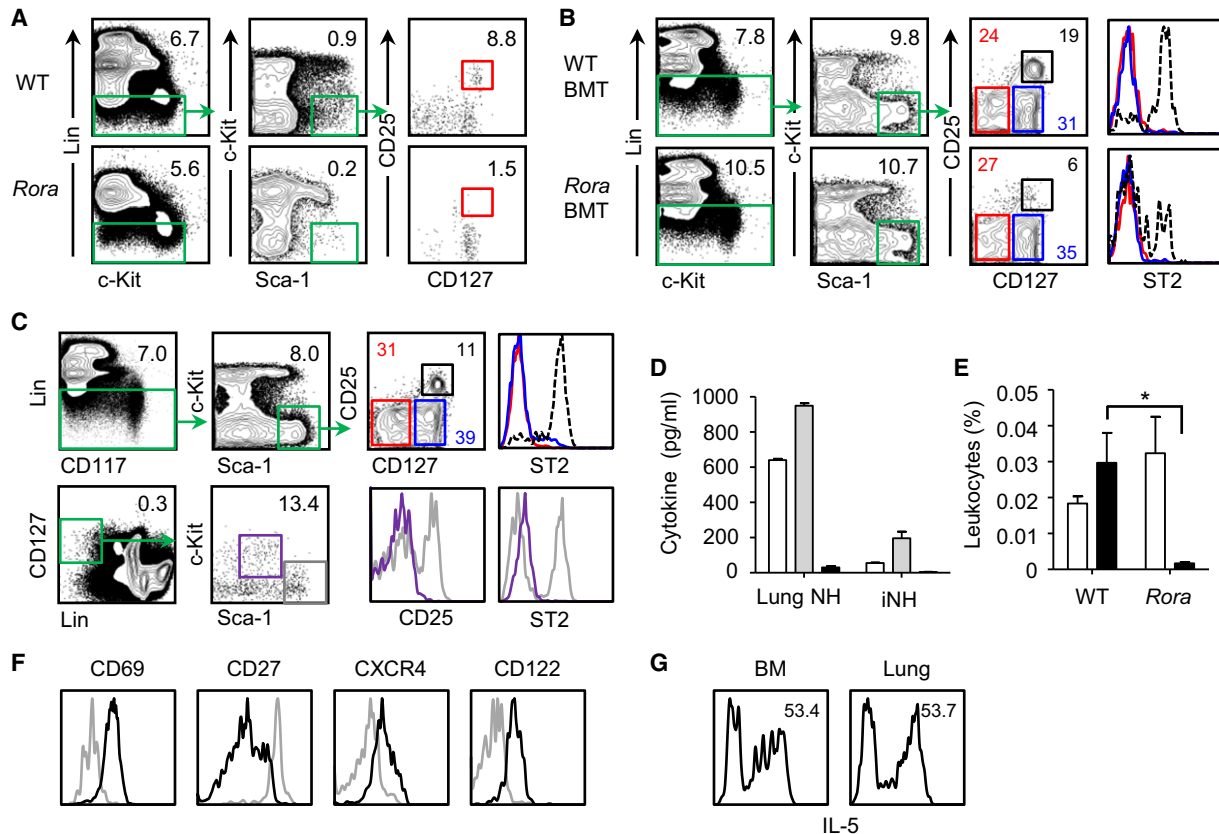
Figure 4. Lin⁻Sca-1^hic-Kit⁻ Cells Contain *Rora*-Dependent CD127⁺CD25⁺ ST2⁺ Immature NH Cells

(A) BM cells from WT and *Rora^sg/sg* littermates were analyzed for Lin⁻Sca-1⁺c-Kit⁻ (LSK⁻) cells (gated by green box) and CD25⁺ CD127⁺ LSK⁻ cells (gated by red box). Numbers show the percentages of gated cells.

(B) BM LSK⁻ cells of WT and *Rora^sg/sg* BMT mice were gated (shown in green boxes) and divided into CD127⁺CD25⁺ (black box), CD127⁺CD25⁻ (blue box), and CD127⁻CD25⁻ (red box) subsets. The expression of ST2 in each subset is shown by histograms. The colors of the histograms correspond to the subsets shown by the gates in the dot plots. Numbers show the percentages of gated cells.

(C) LSK⁻ cells in WT mouse BM were divided into subsets and analyzed for ST2 expression as in (B) (top). Lin⁻CD127⁺Sca-1^loc-Kit^lo CLPs (bottom, purple gates) and LSK⁻ cells (gray gates) in WT mouse BM were identified and analyzed for the expression of CD25 and ST2. The colors of the histograms correspond to the gates in the dot plots. Numbers show the percentages of gated cells.

(D) BM LSK⁻CD127⁺CD25⁺ ST2⁺ (iNH) cells and mature lung NH cells (Lin⁻CD127⁺CD25⁺Sca-1⁺c-Kit^lo) were purified and stimulated for 72 hr with PMA plus ionomycin, and IL-5 (white), IL-13 (gray), or IL-22 (black) production was measured by ELISA.

(E) RGC mice received *Rora^sg/sg* BMT and WT BMT, and iNH cells (black) or CLPs (white) in the BM were analyzed by flow cytometer.

(F) Lung NH cells (black) and BM iNH cells (gray) from normal B6 mice were identified as in (A) and (C), and the expression of CD69, CD27, CXCR4, and CD122 was compared.

(G) BM and lung leukocytes were stimulated for 4 hr with PMA and ionomycin in the presence of Brefeldin A; cell-surface staining and intracellular staining for IL-5 followed. CD45⁺Lin⁻CD127⁺CD25⁺Sca-1⁺ cells were gated, and the percent of IL-5⁺ cells was measured.

For all the flow-cytometry analyses, live (PI⁻ or eFluor780⁻) CD45⁺ leukocytes were gated first. *p < 0.05 (two-tailed Student's t test). Data are representative of three independent experiments (mean and SEM in D and E) (see also Figure S4).

all leukocytes. There was no difference in other donor-derived (CD45.2⁺) leukocyte populations between mice receiving WT BMT and RORα-deficient BMT (Figure S3). These data demonstrate that RORα is critical for the development of NH cells, but not for other lymphocytes.

Immature NH Cells in BM Develop into Mature NH Cells in Mucosal Tissues

Because the above results showed that NH cell development is dependent on RORα, we sought RORα-dependent NH cell progenitors in the BM. Flow-cytometry analysis of BM cells from 3-week-old WT and *Rora^sg/sg* mice showed that the latter

BM had a much smaller population of Lin⁻Sca-1⁺c-Kit⁻ (LSK⁻) cells than did the former (Figure 4A). Given that *Rora^sg/sg* mice live for ~3 weeks and are notably smaller than WT mice, we then analyzed BM cells of RGC mice with WT and *Rora^sg/sg* BMT. WT and *Rora^sg/sg* BMT mice did not drastically differ in the size of the LSK⁻ cell population. However, the LSK⁻ population was heterogeneous and could be divided into CD127⁻CD25⁻, CD127⁺CD25⁻, and CD127⁺CD25⁺ subsets (Figure 4B). In the BM of WT BMT mice, the first two subsets were mostly ST2⁻, whereas the third subset was mostly ST2⁺ and thus closely resembled mature NH cells, but it also contained a small ST2⁻ population. In the BM of *Rora^sg/sg* BMT mice, the

CD127$^+$CD25$^+$ subset was smaller than that of WT BMT mice, and the majority of them did not express ST2. To further characterize Lin$^-$Sca-1$^+$c-Kit$^-$CD127$^+$CD25$^+$ST2$^+$ cells, we compared them with common lymphoid progenitors (CLPs) identified by Lin$^-$CD127$^+$Sca-1^{lo}c-Kit^{lo} (Kondo et al., 1997) in WT mouse BM (Figure 4C). Lin$^-$Sca-1$^+$c-Kit$^-$CD127$^+$CD25$^+$ cells and CLPs were readily distinguished by the expression of Sca-1 and c-Kit (Figure 4C, bottom), and CLPs did not express CD25 or ST2. When purified and stimulated by phorbol ester plus ionomycin, Lin$^-$Sca-1$^+$c-Kit$^-$CD127$^+$CD25$^+$ ST2$^+$ BM cells produced much lower amounts of Th2-cell-type cytokines than did lung or small-intestine NH cells (Figure 4D), indicating their functional immaturity; we therefore termed them iNH cells. $Rora^{sg/sg}$ BMT mice had significantly fewer iNH cells than did WT BMT mice, but they had similar frequencies of CLPs (Figure 4E). When compared to mature lung NH cells from naive WT mice, BM iNH cells expressed less CD69, CXCR4, and CD122 but more CD27 (Figure 4F). Intracellular staining showed that the fraction of IL-5$^+$ cells was similar between BM iNH and lung NH cells (Figure 4G). Purified BM iNH cells and lung NH cells were cultured with IL-33 (10 ng/ml) + IL-25 (10 ng/ml) or IL-33 + TSLP (10 ng/ml) and were then subjected to cell-count and phenotypic analysis (Figures S4A and S4B). Although lung NH cells survived in IL-33 + IL-25, no iNH cells could be detected after 7 days in culture. Conversely, BM iNH cells expanded significantly more in vitro when stimulated with IL-33 and TSLP than did lung NH cells.

To test whether BM iNH cells develop into mature NH cells, we purified iNH cells and transplanted them into Nod-Scid $Il2rg^{-/-}$ (NSG) mice. We also purified Lin$^-$Sca-1^{lo}c-Kit^{lo}CD127$^+$ CLPs, CD127$^-$CD25$^-$cells, and CD127$^+$CD25$^-$ LSK$^-$ cells and injected them into NSG (4,500 cells/mouse) mice for comparison. Three weeks after the injection, donor-derived CD45.2$^+$ NH cells were detected in the small intestine and lungs of the mice injected with iNH cells, whereas they were barely detectable in the mice injected with BM CLPs (Figure 5A). No NH cells were detected in mice injected with CD127$^-$CD25$^-$ cells or CD127$^+$ CD25$^-$ LSK$^-$ cells (data not shown). Although iNH-cell-derived NH cells were detected in significant numbers in the small intestine (Figure 5B) and lungs (Figures 5C and 5D), only very small numbers (~98% less) of CLP-derived NH cells were detected. It should be noted that purified mature lung NH cells repopulate the lung only for a short term and could not be detected after 3 weeks in the injected mice (Halim et al., 2012). To determine whether lung leukocyte isolation conditions adversely affect cells, we treated BM similar to lung tissue, but this did not significantly affect NH cell repopulation (Figures S5A and S5B). We also analyzed donor-derived lymphocytes in the spleen (Figure 5E). As expected, the large majority of CLP-derived cells were B cells, but small numbers of CD4$^+$T cells, CD8$^+$T cells, and NK cells were also detected in the spleen (Figure 5E, black bars). Only very small number of CD8$^+$ T cells and no other donor-derived lymphocytes were detected in the spleen of iNH-cell-injected mice (Figure 5E, white bars). CD127$^-$CD25$^-$ LSK$^-$ BM cells developed into CD4$^+$ and CD8$^+$ T cells (Figure 5E, blue bars), whereas CD127$^+$CD25$^-$ LSK$^-$ cells were similar to CLPs and developed into B, T, and NK cells (Figure 5E, red bars), although they had less B cell potential and more T cell potential than did CLPs. To further investigate the repopulation

dynamics of BM-derived progenitors, we also purified lymphoid primed multipotent progenitors (LMPPs) because they were reported to have greater NH cell potential than were CLPs (Yang et al., 2011). Lin$^-$Sca-1$^+$c-Kit^{hi}Flt3$^+$ LMPPs, Lin$^-$Sca-1^{lo} c-Kit^{lo}Flt3$^+$D127$^+$ CLPs, and iNH cells (Figure S5C) were purified from WT BM and injected into NSG mice (2,500 cells/mouse), and this was followed by analysis of the lungs (Figure S5D) and small intestine (Figure S5E) for NH cell reconstitution. As expected, LMPPs produced slightly higher numbers of NH cells in both tissues than did CLPs. Significantly greater numbers of NH cells were derived from iNH cells in both tissues (Figures S5D and S5E), whereas iNH cells had less capacity to differentiate into other lymphoid lineages than did LMPPs and CLPs (Figure S5F). Besides B and NK cells, low numbers (fewer than 5,000 cells) of T and NKT cells were detected in CLP- and LMPP-injected spleens after 3 weeks.

The BM of NSG mice transplanted with LMPPs, CLPs, or iNH cells was also analyzed after 3 weeks for donor-derived iNH cells (Figure 5F). A minor fraction of LMPP- or CLP-derived cells in the BM of recipients were iNH cells after 3 weeks, whereas the majority of iNH-cell-derived cells were iNH cells. The absolute number of iNH cells derived from CLPs was significantly lower than that of LMPPs, whereas significantly more iNH cells were recovered in the BM of NSG mice injected with iNH cells than in that of mice injected with CLPs or LMPPs (Figure 5G).

NH-Cell-Deficient Mice Have Defective Inflammatory Responses to Allergens

The in vivo function of NH cells as a source of innate Th2-cell-type cytokines has been established primarily through adoptive transfer of in-vitro-expanded NH cells into lymphodeficient RGC or $Il17rb^{-/-}$ mice (Halim et al., 2012; Moro et al., 2010; Neill et al., 2010; Saenz et al., 2010) or selective depletion of NH cells from T-NKT-B-cell-deficient RAG-deficient mice (Chang et al., 2011; Halim et al., 2012; Monticelli et al., 2011). However, the importance of NH cells in the presence of the adaptive immune system is still unclear. Therefore, we tested the effects of intranasal administration of protease allergen papain on RGC mice receiving $Rora^{sg/sg}$ BMT; these mice are NH cell deficient but have normal T cells. As in our previous study (Halim et al., 2012), daily intranasal administration of papain induced severe and acute eosinophilic lung inflammation in control WT BMT mice. Eosinophils were detected in the lung lavage (Figure 6A) and lung tissue (Figure 6B) of WT BMT mice treated with papain, but not with heat-inactivated papain. In contrast, eosinophil infiltration was almost undetectable in $Rora^{sg/sg}$ BMT mice. WT BMT and $Rora^{sg/sg}$ BMT mice did not significantly differ in papain-induced neutrophil infiltration into lung lavage (Figure 6C). They also had the same numbers of other leukocytes—including CD4$^+$ T cells, NK cells, and B cells—in the lungs, and papain-treatment did not change the leukocyte numbers other than neutrophils (Figure 6D). Papain-induced mucus hyperproduction was also notably lower in $Rora^{sg/sg}$ BMT mice than in WT BMT mice (Figure 6E). We also tested IL-25-induced peritoneal inflammation. Intraperitoneal injection of IL-25 induced eosinophil infiltration into the peritoneal cavity and mucus production in the small intestine of WT BMT mice, whereas those inflammatory responses were greatly reduced in $Rora^{sg/sg}$ BMT mice (Figure S6). Comprehensive analysis of leukocytes in the peritoneal
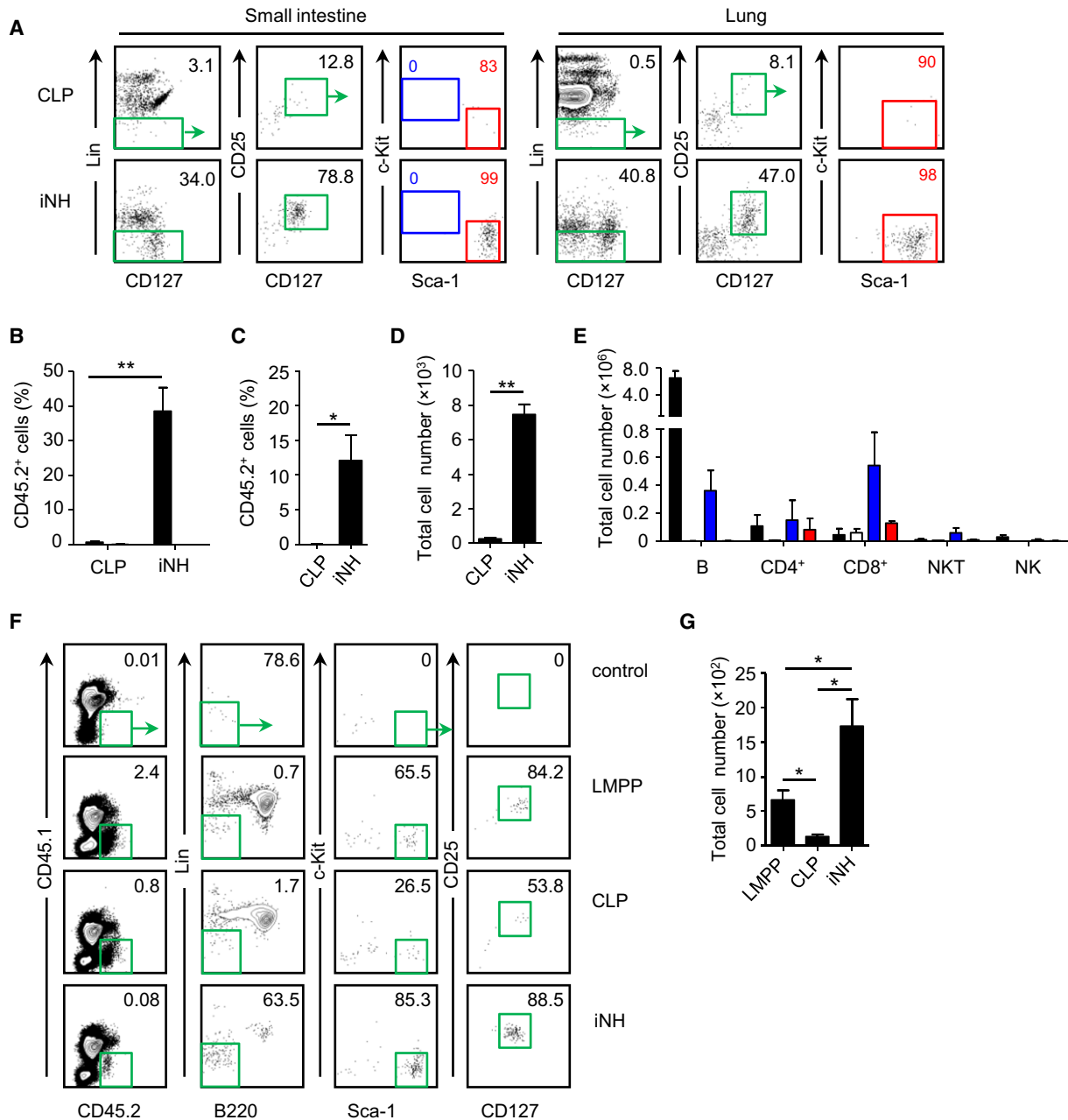
Figure 5. iNH Cells Are More NH-Cell-Lineage Restricted and Efficient than LMPPs or CLPs When Generating NH Cells

(A) CLPs and iNH cells were purified by cell sorting from WT B6 mouse BM, and 4,500 cells per mouse were transplanted into Nod-Scid $Il2rg^{-/-}$ (NSG) mice. Mice were analyzed for donor-derived NH cells (red) and RORγt[+] ILCs (blue) in the small intestine and lungs after 3 weeks. Numbers are the percentages of gated cells among live (DAPI[−]) CD45.2[+] donor leukocytes.

(B and C) The percentages of donor-derived NH cells (black bar) or RORγt[+] ILCs (white bar) in the small intestine (B) and lungs (C) in multiple experiments are shown.

(D) Absolute numbers of donor-derived mature NH cells in the lungs were calculated.

(E) Donor-derived lymphocytes in the spleen of NSG mice injected with iNH cells (white), CLPs (black), LSK^{−}CD127^{+}CD25^{−} ST2^{−} cells (blue), or LSK^{−}CD127^{−}CD25^{−} ST2^{−} cells (red) were identified by flow cytometry and quantified.

(F) The BM of NSG mice injected with nothing (control), LMPPs, CLPs, or iNH cells (2,500 cells per mouse) was analyzed 3 weeks after adoptive transplant for iNH cells. Numbers show the percentages of gated cells. Live (PI^{−}) cells were gated first.

(G) The absolute number of donor-derived iNH cells in the BM (left femur and tibia) of the transplanted mice in (F) was calculated.

*p < 0.05, **p < 0.001 (two-tailed Student's t test). Data are representative of three independent experiments (mean and SEM in B–E and G) (see also Figure S5).

lavage showed no difference in macrophages (Figure 6F), neutrophils, dendritic cells, basophils (Figure 6G), B cells, NK cells, NKT cells, or T cells (Figure 6I) between WT and *Rora*[sg/sg] BMT mice treated with IL-25 (see also Figure S6). These results indicate that even in the presence of intact Th2 cells, NH cells are required for allergen-induced acute eosinophilic inflammation.
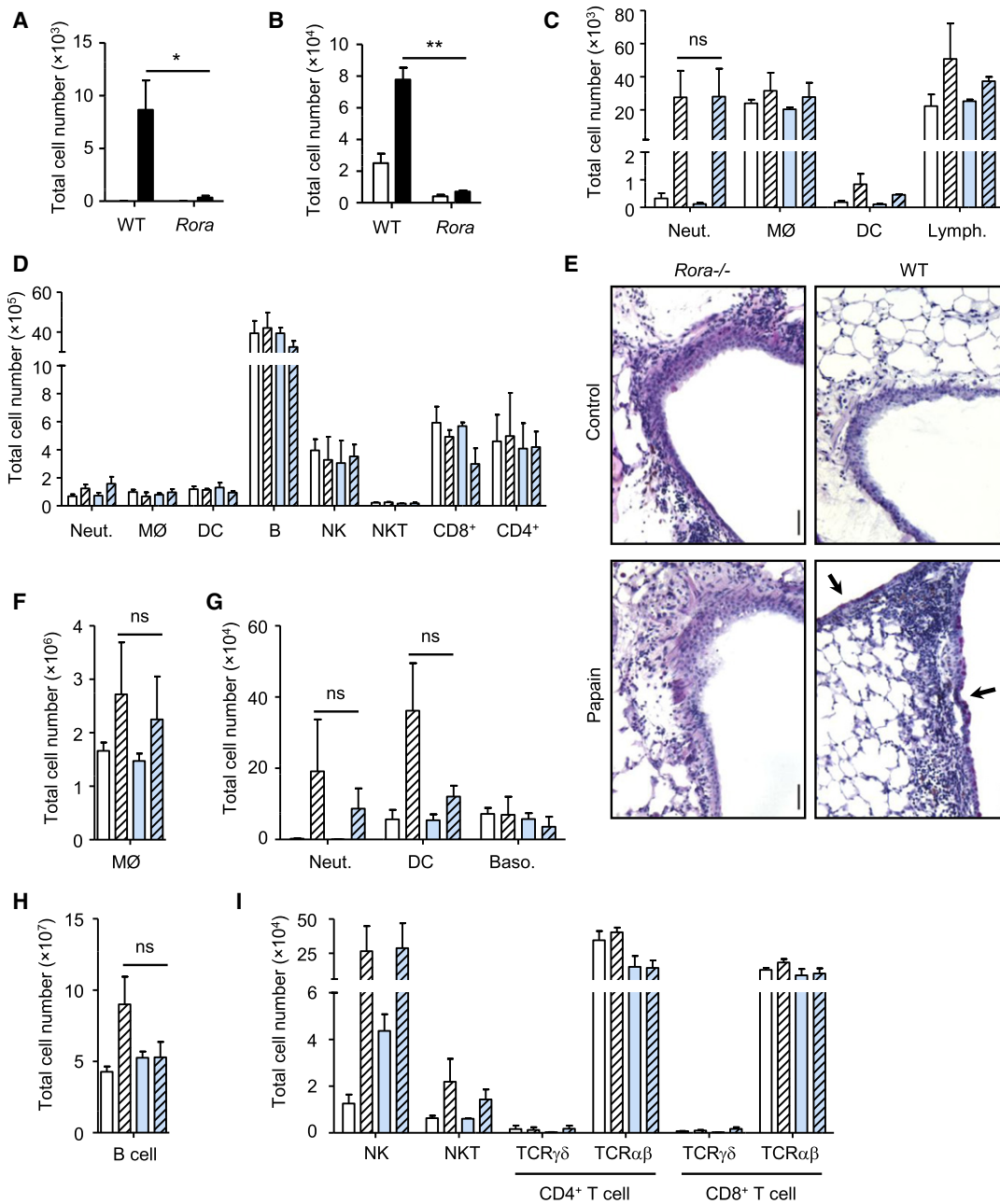
Figure 6. NH-Cell-Deficient _Rora^sg/sg_ BM Chimeras Have an Impaired Innate Th2-Cell-Type Response

(A) _Rag2^−/−Il2rg^−/−_ (RGC) mice reconstituted with _Rora^sg/sg_ (_Rora_) or WT BM received three consecutive daily intranasal administrations of the protease allergen papain (black bars) or heat-inactivated papain (white bars), and bronchioalveolar lavage was prepared on day 4. Eosinophils in the lavage were identified by flow cytometry and quantified.

(B) Eosinophils in the lung tissue of the mice in (A) were identified by flow cytometry and quantified. White bars show those in mice treated with heat-inactivated papain, and black bars show those in mice treated with papain.

(C) Indicated leukocytes in bronchioalveolar lavage prepared from WT (white) or _Rora^sg/sg_ (blue) BMT mice as in (A) were identified by flow cytometry. Results of control mice treated with heat-inactivated papain (no stripes) and mice treated with papain (stripes) are shown.

(D) Indicated leukocytes in the lung tissues of WT (white) or _Rora^sg/sg_ (blue) BMT mice as in (A) were analyzed and quantified by flow cytometry. Results of control mice treated by heat-inactivated papain (no stripes) and mice treated with papain (stripes) are shown.

(E) RGC mice reconstituted with _Rora^sg/sg_ (_Rora_) or WT BM were treated with papain as in (A), and mucus production in the lungs was analyzed by PAS staining. Black arrows show mucus. The scale bar represents 50 μm.

(F–I) RGC mice reconstituted with _Rora^sg/sg_ or WT BM were challenged by three daily intraperitoneal administrations of IL-25 or PBS control. Macrophages (F), neutrophils, DCs, basophils (G), B cells (H), and other indicated lymphocytes (I) were identified in the peritoneal lavage by flow cytometry in WT (white) or _Rora^sg/sg_ (blue) BMT mice treated with the control (no stripes) or IL-25 (stripes).

*p < 0.05, **p < 0.001 (two-tailed Student's t test). Data are representative of three independent experiments (mean and SEM in A–D and F–I) (see also Figure S6).

DISCUSSION

NH cells and RORγt[+] ILCs represent two populations of innate lymphocytes whose primary function is to produce cytokines. NH cells are stimulated by combinations of IL-33, IL-25, TSLP, and IL-7 (Halim et al., 2012; Moro et al., 2010; Neill et al., 2010; Saenz et al., 2010) and produce IL-5 and IL-13, whereas RORγt^{+} ILCs are stimulated by IL-23 and produce IL-22 and IL-17A. Although both share the phenotype of Lin^{−}CD127^{+}CD25^{+}, the lineage relationship between the two innate lymphocyte populations has been unclear. In the current study, innate lymphocytes (Lin^{−}CD127^{+}CD25^{+}) have been divided into two distinct subsets, namely Sca-1^{+}c-Kit^{lo} NH cells and Sca-1^{−}c-Kit^{+} RORγt^{+} ILCs. This allows simultaneous analysis of the two innate lymphocyte populations in multiple tissues, including the lungs, small and large intestines, and MLNs. Although both populations were found in the intestines and MLNs, naive mouse lungs had NH cells, but not RORγt[+] ILCs. Our analysis of mutant mice deficient in RORα or RORγt, two members of the ROR family of transcription factors, has shown that they differentially regulate the development of the two innate lymphocyte populations in all tissues examined. RORα is critical for NH cells, but not for RORγt[+] ILCs, whereas RORγt is required for RORγt[+] ILCs, but not for NH cells, as previously reported (Eberl et al., 2004; Sanos et al., 2009; Sawa et al., 2010). In addition, we have identified possible NH-cell-committed progenitors (iNH cells) that are distinct from CLPs. These iNH cells have the capacity to develop into mature NH cells, but not RORγt[+] ILCs.

Our finding with RORα-deficient mice is consistent with a very recent report by Wong et al., who have also shown that RORα is critical for nuocyte development (Wong et al., 2012). In their study, nuocytes identified in MLNs by Lin[−]ICOS[+] ST2^{+} produced IL-5 and IL-13 upon stimulation, and they are therefore likely to be identical to MLN NH cells observed in our study. We have shown that RORα-deficient, but not RORγt-deficient, mice have very few NH cells in the lungs, small intestine, and large intestine. We have also found that NH cells in the small intestine of naive WT mice do not express ST2, which is often used as a marker for NH cells. We have not been able to detect a substantial number of NH cells or RORγt[+] ILCs in the lungs and intestines of NSG mice injected with BM CLPs. Instead, we have found that NH cells are generated much more efficiently from NH-like cells termed iNH cells, which are among the LSK^{−} BM cells. LSK^{−} cells have been known to have no long-term repopulation capacity, are phenotypically and functionally heterogeneous, and contain early-lymphoid committed progenitors (Kumar et al., 2008). Although iNH cells resemble mature NH cells, their cell-surface expression of CD27 is higher than that of lung NH cells. CD27 is found on hematopoietic stem cells and lymphoid progenitors, and its expression is also known to decrease during the maturation of other innate lymphocytes (Gascoyne et al., 2009). Conversely, iNH cells express less CD69, CXCR4, and CD122 than do mature lung NH cells in naive mice. Furthermore, on a per-cell basis, iNH cells produce much smaller amounts of Th2-cell-type cytokines upon stimulation by phorbol myristate acetate (PMA) plus ionomycin and differ from mature lung NH cells in their response to different cytokine stimulation in vitro. When injected into nonirradiated NSG mice, iNH cells amplified, were found in the BM, and became NH cells in the lungs and intestines. It should be noted that mature NH cells isolated from the lungs and injected into NSG mice did not expand or persist in the mice (data not shown). Interestingly, a subset of iNH cells in the BM seemed to be RORα independent given that we detected a small number of iNH cells in the BM of RGC mice injected with *Rora*[sg/sg] BM cells. They might be progenitors for iNH cells that require RORα for further differentiation into iNH cells.

CLPs in our study are defined by Lin^{−}CD127^{+}-expressing intermediate amounts of Sca-1 and c-Kit (Kondo et al., 1997), and approximately 70% of this population expresses Flt3. When injected into nonirradiated NSG mice, they efficiently develop into splenic T, B, and NK cells and a very small number of NH cells. Wong et al. isolated Lin^{−}CD127^{+}Flt3^{+} BM cells as CLPs and induced differentiation into nuocytes in vitro (Wong et al., 2012). When the same CLP population was injected into irradiated CD45-congenic mice, donor-derived nuocytes were not detected in the MLNs unless IL-25 was injected. Thus, CLPs might have residual potential for NH cell differentiation, but they do not seem to be the main source of NH cells in vivo. Recent work by the Bhandoola laboratory also showed that CLPs have only limited NH cell potential, whereas immature Lin[−]Sca-1^{+}c-Kit[hi]Flt3^{+} LMPPs more efficiently develop into NH cells in the lungs (Yang et al., 2011). Our results confirmed that LMPPs are indeed more efficient than Lin^{−}CD127^{+}Flt3^{+} CLPs at generating NH cells, and we furthermore showed that iNH cells have significantly more robust potential for NH cell differentiation than do either CLPs or LMPPs. We have also shown that although LMPPs give rise to significantly more iNH cells in the BM after transplantation than do CLPs, the number of iNH cells that expand after adoptive transfer is also significantly more than that of both CLPs and LMPPs. Furthermore, CLPs and LMPPs by definition are not committed to a single lineage, as seen by the small fraction of iNH cells generated in the BM and the presence of other lymphocytes detected in the spleen, whereas injected iNH cells appear to be highly restricted to a NH cell fate. As such, it appears likely that CLPs, as currently defined, are heterogeneous, and a minor fraction retains NH cell potential. Because LMPPs are thought to be upstream of CLPs in lymphocyte development (Adolfsson et al., 2001), the results suggest that the majority of iNH cells develop from LMPPs, whereas CLPs contribute to iNH cell development to a lesser extent.

Rora is highly expressed in Th17 cells, which also express *Rorct* (Ivanov et al., 2006; Yang et al., 2008). *Rora*[sg/sg] mouse spleen CD4^{+} T cells show significantly lower Th17 responses than do those of WT mice (Yang et al., 2008). However, *Rora*[sg/sg] mice are much smaller and have much fewer lymphocytes in general, and they do not live much longer than 3 weeks after birth. Transplantation of BM cells from *Rora*[sg/sg] RORγt-deficient and double deficient mice into RAG-deficient mice showed that RORα-deficiency has only a minor effect on Th17 cell differentiation. Although RORγt is more critical for Th17 cells, deficiency of both RORα and RORγt almost completely inhibits Th17 cell differentiation (Yang et al., 2008). Unlike Th17 cells, NH cells do not express RORγt, and RORα-deficiency alone is sufficient to impair NH cell development, as demonstrated by the lack of NH cells in the lungs and intestines of RGC mice receiving *Rora*[sg/sg] BMT. Importantly, no other defects were detected in these mice, and other Th2 cell responses appeared normal.

Nevertheless, these mice did not mount an eosinophilic lung inflammatory response to the protease allergen papain, which is mediated by Th2-cell-type cytokines. Therefore, the data suggest that NH cells are critical for acute allergic inflammation even in the presence of an otherwise intact Th2 cell response. Interestingly, *Rora^sg/sg* mice also have an attenuated Th2 cell response to OVA-induced airway inflammation (Jaradat et al., 2006). In humans, *RORA* has been found to be one of several asthma-associated genes (Moffatt et al., 2010). Previous studies have shown that NH cells are a critical source of Th2-cell-type cytokines in RAG-deficient mice, but the in vivo role of NH cells in normal mice is still unclear. Further studies of NH-cell-deficient mice generated by *Rora^sg/sg* BMT into RGC mice will most likely reveal the importance of NH cells in allergic diseases, including asthma, in the presence of an intact adaptive immune system.

EXPERIMENTAL PROCEDURES

Mice

C57BL/6, C57Bl/6.Pep3b, NOD-SCID, and NOD-SCID *Il2rg^−/−* mice were maintained in the British Columbia Cancer Research Centre (BCCRC) pathogen-free animal facility. B6.129P2(Cg)-*Rorc^tm2Litt*/J and B6.Cg-*Rora^sg*/J mice were purchased from The Jackson Laboratories. B6.*Rag2^−/−Il2rg^−/−* mice were purchased from Taconic Farms. Mice were used at 4–8 weeks of age. All animal use was approved by the animal care committee of the University of British Columbia, and animals were maintained and euthanized under humane conditions in accordance with the guidelines of the Canadian Council on Animal Care.

Genotyping and qPCR

Pups from *Rora^sg/+* breeders were genotyped with DNA obtained from ear notches before experiments. Primer sequences and PCR protocol were obtained from The Jackson Laboratories online database. Prior to performing relative quantification of *Rora* in the described NH cells, we consulted the BioGPS database to gain an appreciation for potential tissues to use as positive controls; using RT-PCR, we confirmed expression of *Rora* in primary B6 liver. For subsequent qPCR experiments, RNA was isolated from fluorescence-activated cell sorting (FACS)-purified B6 NH cells, expanded in vitro with IL-25 and IL-33 for 3 days in CD4+ T cells isolated from B6 spleen with the EasySep negative selection kit (StemCell) or from primary B6 liver with the RNAeasy Mini Kit (QIAGEN), treated by the Turbo DNase-free kit (Ambion), and reverse transcribed with Superscript III (Invitrogen). All procedures were performed as indicated by the manufacturers. Necessarily, the primer pairs for *Rora* (RORα forward: 5′-GAGCTCCAGCAGATAACGTG-3′; RORα reverse: 5′-GCAAACTCCACCACATACTGG-3′) and β-actin (β-actin forward: 5′-AAGGCCAACCGTGAAAAGAT-3′; β-actin reverse: 5′-GTGGTACGACCA GAGGCATAC-3′) were first found to amplify equally efficiently. The comparative C_T method was employed for determining *Rora* expression across the indicated cell types and tissues with the use of the POWER SYBR Green Master Mix (ABI) in an ABI 7500 Real Time System (Applied Biosystems) under default reaction conditions.

BMT

B6.*Rag2^−/−Il2rg^−/−* mice were sublethally irradiated (350 Rads) and subsequently received intravenous transplantation of 10^7 whole BM cells from 4-week-old WT or *Rora^sg/sg* mice. B6.Pep3b mice were lethally irradiated (1,000 Rads) and received transplantation of 10^7 whole BM cells from 4-week-old WT or *Rora^sg/sg* mice. Mice were given Ciprofloxacinand HCL for 4 weeks and were used for analysis 8–16 weeks after transplantation.

Antibodies, Reagents, FACS Sorting, and Analysis

FITC-conjugated CD3ε, CD19, B220, NK1.1, Mac-1, Gr-1, Ter119, and CD45.2 antibodies; phycoerythrobilin (PE)-conjugated CD3, CD127, and RORγt antibodies; PE.Cy5-conjugated CD127; PerCP-Cy5.5 conjugated CD19, CD25, NK1.1, and CD3 antibodies; PE.Cy7-conjugated Sca-1 and

DX5; allophycocyanin (APC)-conjugated CD117, CD25, and FcεR1α antibodies; APC-eFluor780-conjugated B220; Alexa Fluor 700-conjugated CD45.2 and CD11c; eFluor 450-conjugated CD3ε, CD19, B220, NK1.1, Gr-1, CD11b, Ter119, and NKp46; eFluor 605NC-conjugated CD4; and eFluor 650NC-conjugated Thy1.2 were purchased from eBioscience. FITC-conjugated 7/4 was purchased from Abcam. FITC-conjugated CD69 and CD127; PE-conjugated NKp46, CD27, CXCR4, CD122, Flt3, ICOS, IL-13, and Siglec-F antibodies; APC-conjugated IL-5; and BD Horizon V500-conjugated CD45 were purchased from BD Bioscience. FITC-conjugated anti-ST2 was purchased from MD Bioproducts. Propidium iodide (PI), eFluor 780 (eBioscience), or DAPI reagents were used for excluding nonviable cells. IL-2, IL-4, IL-7, IL-23, IL-25, IL-33, and TSLP were purchased from eBioscience; Papain, PMA, and ionomycin were purchased from Sigma Aldrich. BD Fortessa, BD Caliber (Cytek 6 color upgrade), and Canto II were used for phenotypic analysis; BD FACS Aria II was used for cell sorting and phenotypic analysis. Flowjo v.8.6 was used for data analysis.

Primary Leukocyte Preparation

Cell suspensions were prepared from the lungs, spleen, MLNs, or BM as described (Veinotte et al., 2008). Small and large intestines were dissected and flushed with cold PBS and were cut longitudinally and washed with cold PBS. BM or washed intestines were cut into small pieces with a razor and digested for 40 min in MEM, 10% FBS, penicillin and streptomycin (P+S), 50 mM 2-mercaptoethanol (2ME), Collagenase IV (Invitrogen), and DNase (Sigma) at 37°C. Digested tissue was pushed through a 70 μm strainer, and Percoll (GE Healthcare) gradient enrichment of leukocytes followed.

Isolation of NH Cells, iNH Cells, CLPs, and LMPPs

Single cells were incubated with 2.4G2 for blocking Fc receptors; were stained with FITC-conjugated lineage marker mAbs (CD3, CD19, B220, NK1.1, Mac-1, GR-1, and Ter119), PE-conjugated CD127, PerCP-Cy5.5-conjugated CD25, PE.Cy7-conjugated Sca-1, APC-conjugated CD117, and Alexa 700-conjugated CD45.2; and were purified by FACS. BM was stained with FITC-conjugated ST2, PE-conjugated CD127, PerCP-Cy5.5-conjugated CD25, PE.Cy7-conjugated Sca-1, APC-conjugated CD117, Alexa 700-conjugated CD45.2, and eFluor 450-conjugated lineage marker mAbs (CD3, CD19, B220, NK1.1, Mac-1, GR-1, and Ter119) and was purified by FACS. A total of 4,500 CLPs or iNH cells were injected into nonirradiated NSG mice via the tail vein. For LMPP, CLP, and iNH cell isolation, BM was stained with FITC-conjugated CD127, PE-conjugated Flt3, PerCP-Cy5.5-conjugated CD25, PE.Cy7-conjugated Sca-1, APC-conjugated CD117, APC-eFluor780-conjugated B220, eFluor 450-conjugated lineage marker mAbs (CD3, CD19, NK1.1, Mac-1, GR-1, and Ter119), and V500-conjuaged CD45.2 and was purified by FACS. A total of 2,500 LMPPs, CLPs, or iNH cells were injected into nonirradiated NSG mice via the tail vein.

Cytokine Production Assay

Flow-cytometry-purified cells were cultured in 200 μl RPMI-1640 media containing 10% FBS, P+S, and 2 ME at 37°C. Cells were stimulated with IL-33 (10 ng/ml), PMA (30 ng/ml), ionomycin (500 ng/ml), IL-23 (10 ng/ml), IL-7 (10 ng/ml), TSLP (10 ng/ml), and IL-33 (10 ng/ml).

In Vitro CD4+ T Cell Stimulation

Spleen CD4+ T cells were enriched with negative selection by EasySep (StemCell) and were stimulated as described (McKenzie et al., 1998).

Intestine Explant Culture

Mice were sacrificed by CO_2 asphyxiation. Intestines were dissected, flushed with cold PBS, opened longitudinally, and washed in cold PBS. Explants were prepared with a 5 mm biopsy punch. Two explants were placed in 0.5 ml RPMI-1640, 10% FCS, 2 ME, and P+S and were stimulated with IL-25 (10 ng/ml) or IL-23 (10 ng/ml).

Intracellular Staining

Intracellular staining for RORγt was performed with the Foxp3 intracellular staining kit (eBioscience) according to the manufacturer's protocol. Intracellular staining for IL-5 was performed with the Cytofix/Cytoperm kit (BD Biosciences). Dead cells were stained with eFluor 780 (eBioscience)

fixable viability dye before fixation and permeabilization and were excluded during analysis.

ELISAs

IL-5, IL-13, and IL-22 (eBioscience) enzyme-linked immunosorbent assays (ELISAs) were performed according to the manufacturer's protocol.

RNA Isolation and Microarray

Total RNA was isolated from FACS-purified unstimulated cells by Trizol (Invitrogen). Agilent Bioanalyzer 2100, RNA amplification, and microarray services were performed by McGill University and Génome Québec Innovation Centre with Affymetrix Mouse Gene 1.0 arrays. Data analysis was performed with FlexArray 1.5 (Génome Québec). Microarray data sets for other cells were obtained from data assembled by the ImmGen consortium (Heng et al., 2008).

In Vivo Papain Stimulation

Mice were anesthetized by isofluorane inhalation and were then intranasally injected with papain or heat-inactivated papain (10 μg) in 40 μl of PBS on days 0–2. Mice were sacrificed on day 3, and lung and BAL cells (1 ml PBS) were collected or airways were instilled with 50:50 Tissue-Tek OCT Compound and PBS (Adwin Scientific) and fixed in formalin. Lung tissue was processed as described previously; lung and BAL cells were then counted and identified by FACS. Fixed tissues were embedded in paraffin and processed for H&E or PAS (+/− diastase) staining by the Centre for Translational and Applied Genomics (Vancouver, Canada).

Statistics

Data were analyzed with GraphPad Prism 5 (GraphPad Software). A Student's t test was used for determining statistical significance between groups; $p \le 0.05$ was considered significant. The statistical analysis of microarray results was carried out with FlexArray (Genome Quebec).

SUPPLEMENTAL INFORMATION

Supplemental Information includes Supplemental Experimental Procedures and six figures and can be found with this article online at http://dx.doi.org/10.1016/j.immuni.2012.06.012.

REFERENCES

Adolfsson, J., Borge, O.J., Bryder, D., Theilgaard-Mönch, K., Astrand-Grundström, I., Sitnicka, E., Sasaki, Y., and Jacobsen, S.E.W. (2001). Upregulation of Flt3 expression within the bone marrow Lin(-)Sca1(+)c-kit(+) stem cell compartment is accompanied by loss of self-renewal capacity. Immunity 15, 659–669.

Bakalian, A., Kopmels, B., Messer, A., Fradelizi, D., Delhaye-Bouchaud, N., Wollman, E., and Mariani, J. (1992). Peripheral macrophage abnormalities in mutant mice with spinocerebellar degeneration. Res. Immunol. 143, 129–139.

Chang, Y.J., Kim, H.Y., Albacker, L.A., Baumgarth, N., McKenzie, A.N., Smith, D.E., Dekruyff, R.H., and Umetsu, D.T. (2011). Innate lymphoid cells mediate influenza-induced airway hyper-reactivity independently of adaptive immunity. Nat. Immunol. 12, 631–638.

Eberl, G., Marmon, S., Sunshine, M.J., Rennert, P.D., Choi, Y., and Littman, D.R. (2004). An essential function for the nuclear receptor RORgamma(t) in the generation of fetal lymphoid tissue inducer cells. Nat. Immunol. 5, 64–73.

Fujieda, H., Bremner, R., Mears, A.J., and Sasaki, H. (2009). Retinoic acid receptor-related orphan receptor alpha regulates a subset of cone genes during mouse retinal development. J. Neurochem. 108, 91–101.

Gascoyne, D.M., Long, E., Veiga-Fernandes, H., de Boer, J., Williams, O., Seddon, B., Coles, M., Kioussis, D., and Brady, H.J. (2009). The basic leucine zipper transcription factor E4BP4 is essential for natural killer cell development. Nat. Immunol. 10, 1118–1124.

Gold, D.A., Baek, S.H., Schork, N.J., Rose, D.W., Larsen, D.D., Sachs, B.D., Rosenfeld, M.G., and Hamilton, B.A. (2003). RORalpha coordinates reciprocal signaling in cerebellar development through sonic hedgehog and calcium-dependent pathways. Neuron 40, 1119–1131.

Halim, T.Y., Krauss, R.H., Sun, A.C., and Takei, F. (2012). Lung natural helper cells are a critical source of Th2 cell-type cytokines in protease allergen-induced airway inflammation. Immunity 36, 451–463.

Heng, T.S., and Painter, M.W.; Immunological Genome Project Consortium. (2008). The Immunological Genome Project: networks of gene expression in immune cells. Nat. Immunol. 9, 1091–1094.

Ivanov, I.I., McKenzie, B.S., Zhou, L., Tadokoro, C.E., Lepelley, A., Lafaille, J.J., Cua, D.J., and Littman, D.R. (2006). The orphan nuclear receptor RORgammat directs the differentiation program of proinflammatory IL-17+ T helper cells. Cell 126, 1121–1133.

Jaradat, M., Stapleton, C., Tilley, S.L., Dixon, D., Erikson, C.J., McCaskill, J.G., Kang, H.S., Angers, M., Liao, G., Collins, J., et al. (2006). Modulatory role for retinoid-related orphan receptor alpha in allergen-induced lung inflammation. Am. J. Respir. Crit. Care Med. 174, 1299–1309.

Kondo, M., Weissman, I.L., and Akashi, K. (1997). Identification of clonogenic common lymphoid progenitors in mouse bone marrow. Cell 91, 661–672.

Kumar, R., Fossati, V., Israel, M., and Snoeck, H.W. (2008). Lin-Sca1+kit- bone marrow cells contain early lymphoid-committed precursors that are distinct from common lymphoid progenitors. J. Immunol. 181, 7507–7513.

McKenzie, G.J., Emson, C.L., Bell, S.E., Anderson, S., Fallon, P., Zurawski, G., Murray, R., Grencis, R., and McKenzie, A.N. (1998). Impaired development of Th2 cells in IL-13-deficient mice. Immunity 9, 423–432.

Mjösberg, J.M., Trifari, S., Crellin, N.K., Peters, C.P., van Drunen, C.M., Piet, B., Fokkens, W.J., Cupedo, T., and Spits, H. (2011). Human IL-25- and IL-33-responsive type 2 innate lymphoid cells are defined by expression of CRTH2 and CD161. Nat. Immunol. 12, 1055–1062.

Moffatt, M.F., Gut, I.G., Demenais, F., Strachan, D.P., Bouzigon, E., Heath, S., von Mutius, E., Farrall, M., Lathrop, M., and Cookson, W.O.; GABRIEL Consortium. (2010). A large-scale, consortium-based genomewide association study of asthma. N. Engl. J. Med. 363, 1211–1221.

Monticelli, L.A., Sonnenberg, G.F., Abt, M.C., Alenghat, T., Ziegler, C.G., Doering, T.A., Angelosanto, J.M., Laidlaw, B.J., Yang, C.Y., Sathaliyawala, T., et al. (2011). Innate lymphoid cells promote lung-tissue homeostasis after infection with influenza virus. Nat. Immunol. 12, 1045–1054.

Moro, K., Yamada, T., Tanabe, M., Takeuchi, T., Ikawa, T., Kawamoto, H., Furusawa, J., Ohtani, M., Fujii, H., and Koyasu, S. (2010). Innate production of T(H)2 cytokines by adipose tissue-associated c-Kit(+)Sca-1(+) lymphoid cells. Nature 463, 540–544.

Neill, D.R., Wong, S.H., Bellosi, A., Flynn, R.J., Daly, M., Langford, T.K., Bucks, C., Kane, C.M., Fallon, P.G., Pannell, R., et al. (2010). Nuocytes represent a new innate effector leukocyte that mediates type-2 immunity. Nature 464, 1367–1370.

Price, A.E., Liang, H.E., Sullivan, B.M., Reinhardt, R.L., Eisley, C.J., Erle, D.J., and Locksley, R.M. (2010). Systemically dispersed innate IL-13-expressing cells in type 2 immunity. Proc. Natl. Acad. Sci. USA 107, 11489–11494.

Saenz, S.A., Siracusa, M.C., Perrigoue, J.G., Spencer, S.P., Urban, J.F., Jr., Tocker, J.E., Budelsky, A.L., Kleinschek, M.A., Kastelein, R.A., Kambayashi, T., et al. (2010). IL25 elicits a multipotent progenitor cell population that promotes T(H)2 cytokine responses. Nature 464, 1362–1366.

Sanos, S.L., Bui, V.L., Mortha, A., Oberle, K., Heners, C., Johner, C., and Diefenbach, A. (2009). RORgammat and commensal microflora are required for the differentiation of mucosal interleukin 22-producing NKp46+ cells. Nat. Immunol. *10*, 83–91.

Sawa, S., Cherrier, M., Lochner, M., Satoh-Takayama, N., Fehling, H.J., Langa, F., Di Santo, J.P., and Eberl, G. (2010). Lineage relationship analysis of RORgammat+ innate lymphoid cells. Science *330*, 665–669.

Spits, H., and Di Santo, J.P. (2011). The expanding family of innate lymphoid cells: regulators and effectors of immunity and tissue remodeling. Nat. Immunol. *12*, 21–27.

Spits, H., and Cupedo, T. (2012). Innate lymphoid cells: emerging insights in development, lineage relationships, and function. Annu. Rev. Immunol. *30*, 647–675.

Veinotte, L.L., Halim, T.Y., and Takei, F. (2008). Unique subset of natural killer cells develops from progenitors in lymph node. Blood *111*, 4201–4208.

Wong, S.H., Walker, J.A., Jolin, H.E., Drynan, L.F., Hams, E., Camelo, A., Barlow, J.L., Neill, D.R., Panova, V., Koch, U., et al. (2012). Transcription factor RORα is critical for nuocyte development. Nat. Immunol. *13*, 229–236.

Yang, X.O., Pappu, B.P., Nurieva, R., Akimzhanov, A., Kang, H.S., Chung, Y., Ma, L., Shah, B., Panopoulos, A.D., Schluns, K.S., et al. (2008). T helper 17 lineage differentiation is programmed by orphan nuclear receptors ROR alpha and ROR gamma. Immunity *28*, 29–39.

Yang, Q., Saenz, S.A., Zlotoff, D.A., Artis, D., and Bhandoola, A. (2011). Cutting edge: Natural helper cells derive from lymphoid progenitors. J. Immunol. *187*, 5505–5509.